ACS APPLIED NANO MATERIALS

Article

Highly Ordered Titanium Dioxide Nanostructures *via* a Simple One Step Vapor Inclusion Method in Block Copolymer Films

Elsa Coline Giraud, Parvaneh Mokarian- Tabari, Daniel Thomas William Toolan, Thomas Arnold, Andrew J. Smith, Jonathan R Howse, Paul D Topham, and Michael A. Morris

ACS Appl. Nano Mater., **Just Accepted Manuscript** • DOI: 10.1021/acsanm.8b00632 • Publication Date (Web): 18 Jun 2018

ACS Publications

is published by the American Chemical Society. 1155 Sixteenth Street N.W., Washington, DC 20036

Highly Ordered Titanium Dioxide Nanostructures via a Simple One Step Vapor Inclusion Method in Block Copolymer Films

Elsa C. Giraud[†±], Parvaneh Mokarian-Tabari*[±∓], Daniel T. W. Toolan[Δ], Thomas Arnold[§], Andrew J. Smith[§], Jonathan R. Howse[‡], Paul D. Topham[‖], Michael A. Morris[±∓]

† Department of Chemistry, University College Cork, Cork, T12 YN60, Ireland

± Advanced Materials and BioEngineering Research Centre (AMBER) & CRANN, Trinity College Dublin, Dublin 2, Ireland

∓ School of Chemistry, Trinity College Dublin, Dublin 2, Ireland

Δ Department of Chemistry, Dainton Building, University of Sheffield, Sheffield, S3 7HF, UK

‡ Department of Chemical and Biological Engineering, University of Sheffield, Sheffield, S1 3JD, UK

§ Diamond Light Source Ltd, Harwell Science and Innovation Campus, Didcot, OX11 0DE, UK

‖ Aston Institute of Materials Research, Aston University, Birmingham, B4 7ET, UK

KEYWORDS titanium dioxide, titanium tetraisopropoxide, block copolymer, polymer templating, chemical vapor deposition, GISAXS

ABSTRACT: Nanostructured crystalline titanium dioxide (TiO_2) finds applications in numerous fields such as photocatalysis or photovoltaics where its physical and chemical properties depend on its shape and crystallinity. We report a simple method of fabricating TiO_2 nanowires by selective area deposition of titanium tetraisopropoxide (TTIP) and water in a CVD-based approach at low temperature by utilizing a PS-*b*-PEO self-assembled block copolymer thin films as template. Parameters such as exposure time to TTIP (minutes to hours), working temperature (~18 to 40 °C) and relative humidity (20 to 70 %) were systemically investigated through GISAXS, SEM and XPS and optimized for fabrication of TiO_2 nanostructures. The resulting processing conditions yielded titanium dioxide nanowires with a diameter of 24 nm. An extra calcination step (500 °C) was introduced to burn off the remaining organic matrix and introduce phase change from amorphous to anatase in TiO_2 nanowires without any loss in order.

Crystalline and nanocrystalline titanium dioxide (TiO_2), is one of the most studied transition-metal oxides due to its excellent physical and chemical properties. Depending on the TiO_2 polymorph (*i.e.* anatase, rutile and brookite or combinations thereof), TiO_2 nanostructures find applications in various fields such as gas sensing[1,2] photovoltaics[3,4] photocatalysis[5,6] and cell-culture[7].

Methods for forming TiO_2 include chemical and physical vapor deposition (CVD and PVD)[8,9,10], sol-gel[11,12], plasma laser deposition (PLD)[13], atomic layer deposition (ALD and PEALD)[14,15,16,17] and reactive electron beam evaporation[18]. However, those methods (apart from sol-gels) require precision control of gas flow, substrate temperature and working pressure. Although the above mentioned TiO_2 production methods yield highly crystalline films, they require costly equipment and offer poor control over nanostructural arrangement, significantly limiting nanoapplications.

Self-assembled block copolymer (BCP) patterning and/or templating offers a cost-effective approach for the formation of well-defined nanostructured thin film architectures. Block copolymers consist of two (or more) incompatible, covalently bonded polymers that form ordered morphologies with dimensions of sub-10 to 100 nm when phase-separated in the right conditions[19,20,21]. BCP thin films can be used to produce an organic/inorganic hybrid material. The organic component can be subsequently removed, yielding nanostructured inorganic materials[22]. In the past, sol-gel processes have been widely used to form titanium dioxide where a polymer solution and a metal precursor (usually alkoxides) solution are mixed together prior to film coating[23,24,25] or evaporation[26]. A range of different nanostructures (micelles, worm-like, nanowires, nanodots, etc.) may be obtained through controlling a wide range of conditions including sol-gel concentration, solvent, evaporation rate and spin coater speed. However, titanium alkoxide precursors are highly reactive with water and generally require acidic solutions (*e.g.* acetic acid, hydrochloric acid and trifluoroacetic anhydride) to stabilize the precursors and slow down their hydrolysis[27,28]. Evaporation induced self-assembly (EISA) method, among other sol-gel techniques, is a commonly used method for templating inorganic materials. However, obtaining highly ordered nanostructured films *via* this approach remains highly challenging[29]. An alternative, single step fabrication route involves incorporating preformed particles within block copolymer solutions, allowing precise control of the size, shape and crystallinity of the particles. Limited miscibility between the inorganic particles and BCP solutions, however, often results in segregation and is therefore a significant drawback.

Control over nanostructure shapes (nanowires, nanodots, etc.) and, hence, titanium dioxide nanostructures, can be obtained by decoupling block copolymer self-assembly from metal oxide incorporation. BCP templates are used as a scaffold for the formation of inorganic nanostructures[30]. After removal of all organic components, a one-to-one registration is observed between the original pattern and the inorganic counterpart.

The order of resulting oxide is strictly dependent on the film order. For the oxide to selectively incorporate the hydrophilic part of the BCP, a metal precursor solution can be spun cast over the substrate[31]. Alternatively, the pattern may be immersed in metal precursor solution[32]. However, as for sol-gel methods, precise control over metal precursor concentration and stabilization is required.

In this paper, we adapt the former approach (decoupling pattern formation from metal incorporation) by introducing the metal precursors using a CVD-like method. To date, extensive work has been carried out onto PS-*b*-PMMA in CVD, ALD and SIS chambers[33] to form nanostructure materials and thin films[34,35,36]. However, to our knowledge, no attempt using simple evaporation of the precursors under ambient and low temperature has been recorded. Because we aim to selectively deposit inorganic material, PS-*b*-PEO is a block-copolymer of choice for templating, over PS-*b*-PMMA, as hydrophilic functional groups (Ti-O) are capable of bonding with the hydrophilic PEO component[37].

Utilizing the amphiphilic properties of PS-*b*-PEO, its high $\chi_{PS\text{-}PEO}$ value, and the hydrolysis of a titanium alkoxide precursor, we are able to form well-ordered TiO_2 nanostructures without the need of any precise precursor solution formulation or high control over gas flow and pressure. Furthermore, no complex chamber or processing is required as it is for ALD method. The method presented here (although similar to SIS which borrows its chemistries from ALD and consists of cyclic infiltration and reaction), eliminates the sequential steps of the SIS process[34]. All chemicals, including the titanium precursor, are introduced to the chamber at the same time. Highly uniform TiO_2 nanowires and nanodots mimicking the original BCP patterns are produced over large area as evidenced by microscopy analysis. Additionally, this novel approach is both industrially compatible and environmental-friendly. We envisage that the simple, yet highly effective process reported herein may be used widely for selective vapor infiltration of block copolymer domains producing functional inorganic nanostructured materials.

RESULTS AND DISCUSSION

The method used to produce ordered titanium dioxide nanowires is illustrated on **Scheme 1.**

Block Copolymer Self-Assembly. The first stage in this novel CVD-based TiO_2 nanostructure fabrication route utilizes BCP thin films acting as a template for selective adsorption of a TiO_2 precursor. BCP films possess a propensity to self-assemble *via* microphase separation, forming highly ordered nanostructures. PS-*b*-PEO thin films were fabricated *via* spin-coating to produce highly uniform thin films with thicknesses of ~40 nm as measured by ellipsometry (**Figure S1**). As-cast films show poorly ordered films with mixed orientation of PEO cylinders within a PS matrix and, therefore, do not possess a significant degree of long range order that would make them attractive templates for the generation of ordered TiO_2 nanostructures. Solvo-thermal annealing was used to optimize the BCP morphology, where the combination of heat and solvent vapor are employed to promote mobility of the polymer chains, enabling chain re-organization and the formation of morphologies closer to thermodynamic equilibrium. Toluene is a good solvent for the PS domains, allowing the chains to swell and stretch to maximize their contact with the solvent

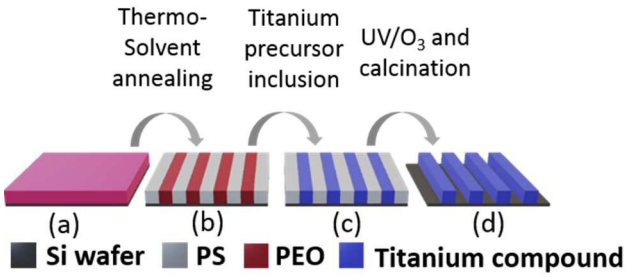

Scheme 1. Illustration of the formation of titanium dioxide nanowires. (a) As-cast thin film of PS-*b*-PEO solution on Si substrate; strate; (b) self-assembled PS-*b*-PEO obtained after thermo-solvent annealing at 60°C in toluene vapors; (c) PS-*b*-PEO thin with SEO/TiO_2 hybrid and (d) titanium dioxide nanowires after UV/O_3 and calcination process.

molecules ($\chi_{PS\text{-}tol}$ = 0.46, $\chi_{PEO\text{-}tol}$ = 5.34, where χ is the solvent-polymer interaction parameter[38,39] and indicates good dissolution if smaller than 0.5). However, at room temperature, the low vapor pressure of toluene (2.9673 kPa)[40] does not provide

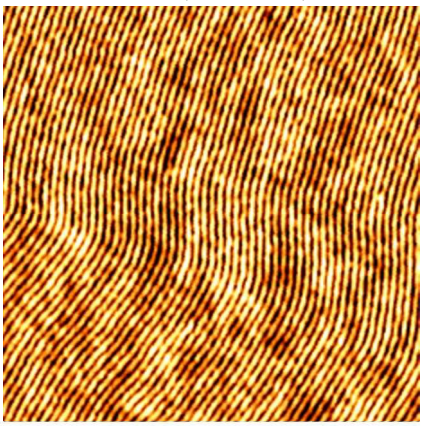

Figure 1. AFM image (2x2 μm) of self-assembled PS-*b*-PEO thin film acting as a template.

enough pressure for the vapors to penetrate the glassy PS film[41] (case II diffusion) and enhance the mobility of the chains. Increasing the temperature to 60 °C increases the vapor pressure to 18.93 kPa, leading to phase separation. On the other hand, water is a good solvent for the PEO[42] domains, due to hydrophilic interactions, and the air moisture in the annealing chamber is sufficient to induce mobility of PEO chains. A topographic AFM image of a BCP film exposed to toluene vapors at 60°C for 2 hours is shown in **Figure 1** where the center-to-center distance was measured to be 38 nm with a line width of 26 nm comparable with dimensions in our previous studies[30,41]. The ability of BCP thin films to adopt different nanoscale morphologies[41] offers routes to generate a range of different TiO_2 nanostructures. **Figure S2** presents vertical arrangement (pillars) of PEO domains within a PS matrix and, after incorporation, subsequent titanium dioxide nanodots.

Titanium dioxide nanostructure fabrication. In order to fabricate TiO_2 nanowires, PS-*b*-PEO thin films with morphologies consisting of cylinders orientated parallel to the surface were used as a template (**Figure 1)** to generate the desired titanium dioxide nanostructures. This was achieved by exposing the BCP thin-films to titanium alkoxide vapors, which

undergo hydrolysis and subsequent condensation to form titanium hydroxides. Titanium alkoxide precursors, known to be susceptible to hydrolysis, are scarcely used in aqueous or humid environments[43] and are often diluted in alcohol prior to use to manage the reaction rate[44]. The two different components of PS-*b*-PEO possess different affinities to titanium alkoxides. PEO has been shown

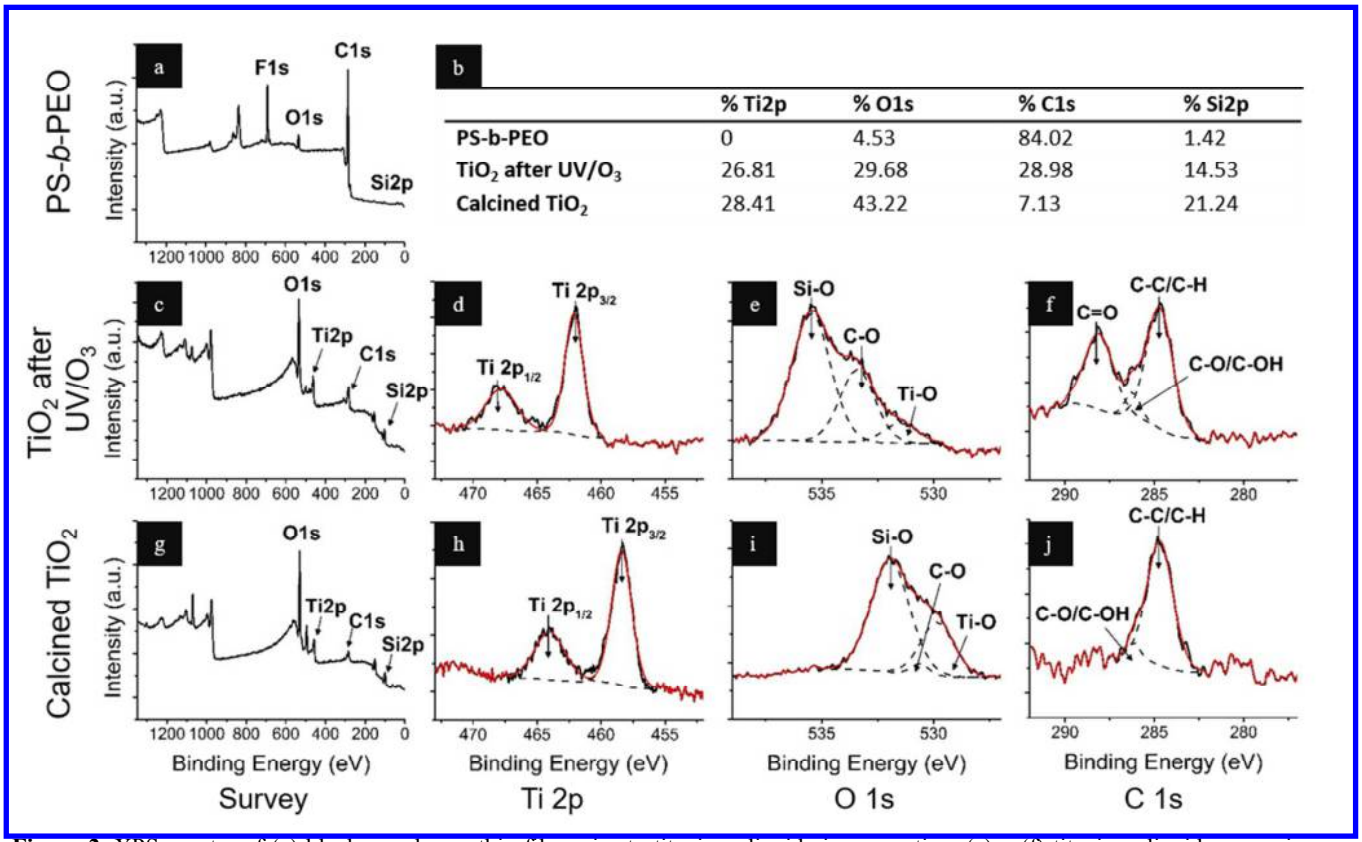

Figure 2. XPS spectra of (a) block copolymer thin film prior to titanium dioxide incorporation, (c) – (f) titanium dioxide nanowires on silicon after UV ozone treatment and before calcination at 500 °C, and (g) – (j) titanium dioxide nanowires on silicon wafer after UV ozone treatment and calcination. High resolution XPS spectra were recorded for Ti 2p core level (d) and (h), O 1s core level (e) and (i), and C 1s core level (f) and (j). Table (b) gives the atomic percentage of each element. Conditions for titanium dioxide formation are as follow: 20 min exposure to TTIP, at 30 ^{0}C and 60 RH.

to have a high affinity for cations due to hydrophilic interaction between cations and oxygen atoms from the PEO domain[45]. On the contrary, the hydrophobic nature of the PS excludes cation incorporation. By exposing the polymer film to pure titanium tetraisopropoxide (TTIP) solution, we aim to selectively deposit Ti^{4+} cations within the PEO domains. After ion incorporation, UV ozone treatment was performed to ensure complete oxidation of the titanium precursor to titanium dioxide and to remove most organic components (TTIP reacting with PEO, it is likely that some PEO remains under TiO_2 domains). The resulting titanium dioxide nanowires, after 3 hours of exposure to TTIP vapors and UV ozone treatment, have a thickness of 12 nm as determined by ellipsometry (**Figure S1**). In the approach presented herein, precise control over the relative humidity (RH) and temperature enables selective generation of TiO_2 onto the PEO domains of the BCP template.

Influence of the precursor. Two different titanium alkoxide precursors were investigated, TTIP and titanium butoxide, which both possess high volatility and high vapor pressure making them suitable for this CVD-based approach. AFM images of titanium dioxide formed under ambient conditions (~18 °C) after 30- to 255-minute exposure to TTIP vapors are available in **Figure S3.** The average line width was measured to be 24 nm (2 nm smaller than the original template)[30] while the average center-to-center distance was 38 nm.

However, when using titanium butoxide, little or no titanium dioxide nanostructures were observed. Although titanium butoxide precursor has a higher vapor pressure than titanium tetraisopropoxide, the long alkane chains of titanium butoxide lower its apparent volatility by increasing the intermolecular forces within the alkyl chains (steric hindrance) and, hence, hinder its interaction with the PEO domains[16]. On the contrary, bulky alkyl groups from TTIP prevented oligomerization and promoted higher volatility.

XPS was used to study the chemical nature of the incorporated titanium precursor after UV/O_3 treatment and after calcination. Data shown here are for titanium dioxide nanowires obtained after 20 min exposure to TTIP, at 30 °C and 60 RH. Recorded surface survey after UV/O_3 treatment and calcination indicated the presence of expected elements (Si, Ti, O) as well as C 1s (286 eV) peaks as shown in **Figure 2 (f) and (j)**. The fluorine peak, only present in the PS-*b*-PEO thin film survey, Error! Reference source not found. **2 (a)**, is believed to be a consequence of cross-contamination. Most organic components are removed following UV ozone treatment, as shown in the **Table (b) of Figure 2**, with a drop in C 1s atomic percentage from 84 to 29 % due to polymer degradation after exposure to UV/O_3. Calcination process at 500 °C, under ambient condi-

tions, is applied to remove even further the remaining traces of the organic matrix. Another drop in C 1s atomic percentage from 29 to 7 % is observed for the same sample (see **Table b** in **Figure 2**). Furthermore, an increase in Si 2p atomic percentage after two hours of calcination at 500 °C is an indirect evidence of removal of the organic matrix as more silicon surface us readily available. As such, the contrast observed in the SEM images (**Figure 3**) reflects the formation of the inorganic TiO_2 nanowires. Extensive Ti 2p spectra, **Figure 2 (d)** and **(h)**, were recorded to analyze with exactitude the titanium chemical environment. The Ti 2p doublet observed is characteristic to Ti^{4+} species in TiO_2 (O–Ti–O bonding)[46,47]. It consists of the Ti $2p_{3/2}$ peak at ~460 eV (462 and 458.5 eV before and after calcination, respectively) and the Ti $2p_{1/2}$ peak at ~466 eV (468 and 464 eV before and after calcination,

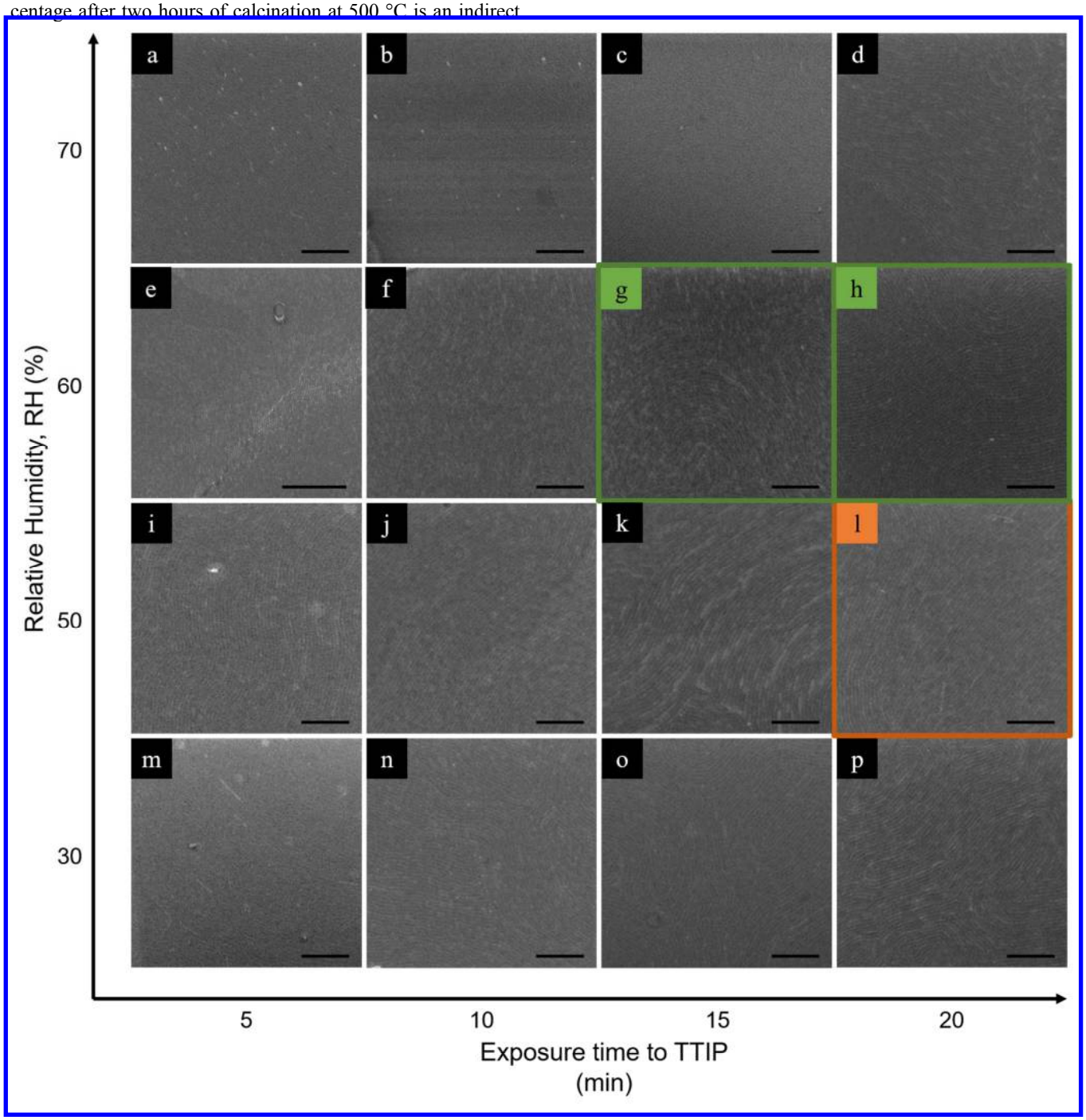

Figure 3. SEM images showing the evolution of formed titanium dioxide nanowires at 30 °C as a function of exposure time to TTIP (x-axis) and relative humidity (y-axis). The self-assemble BCP thin films were exposed to TTIP in 70% relative humidity for (a) 5 min, (b) 10 min, (c) 15 min and (d) 20 min ; in 60% relative humidity for (e) 5min, (f) 10 min, (g) 15 min, (h) 20 min ; in 50% relative humidity for (i) 5 min, (j) 10 min, (k) 15 min and (l) 20 min; in 30% relative humidity for (m) 5 min, (n) 10 min, (o) 15 min and (p) 20 min. All scale bars = 500 nm, except in (e) were scale bar = 1 µm. All images were taken after a 3-hour UV ozone treatment

respectively). The presence of Ti^{3+} and Ti^{2+} species are not observed within experimental error. **Figure 2 (e)** and **(i)** show the core level of O 1s spectra, before and after calcination, which consist of a broad peak. The peaks centered at 531.4 and 529.8 eV, before and after calcination respectively are attributed to titanium dioxide at the surface[48] (Ti-O bonds). Peaks at 535.4 and 531.9 eV are attributed to SiO_2 while peaks at 533.4 and 530.6 eV are attributed to the presence of remaining PEO groups after UV ozone treatment and calcination (C-O and C=O bonds). Presence of the polymer is also confirmed in **Figure 2 (f) and (j)** with peaks at 288.2 and 286.3 eV before calcination, and peak at 286.2 eV after calcination. Adventitious carbon peak was calibrated to be 284.8 eV. Calcination of samples is a requirement to obtain pure titanium dioxides nanostructures supported on SiO_2.

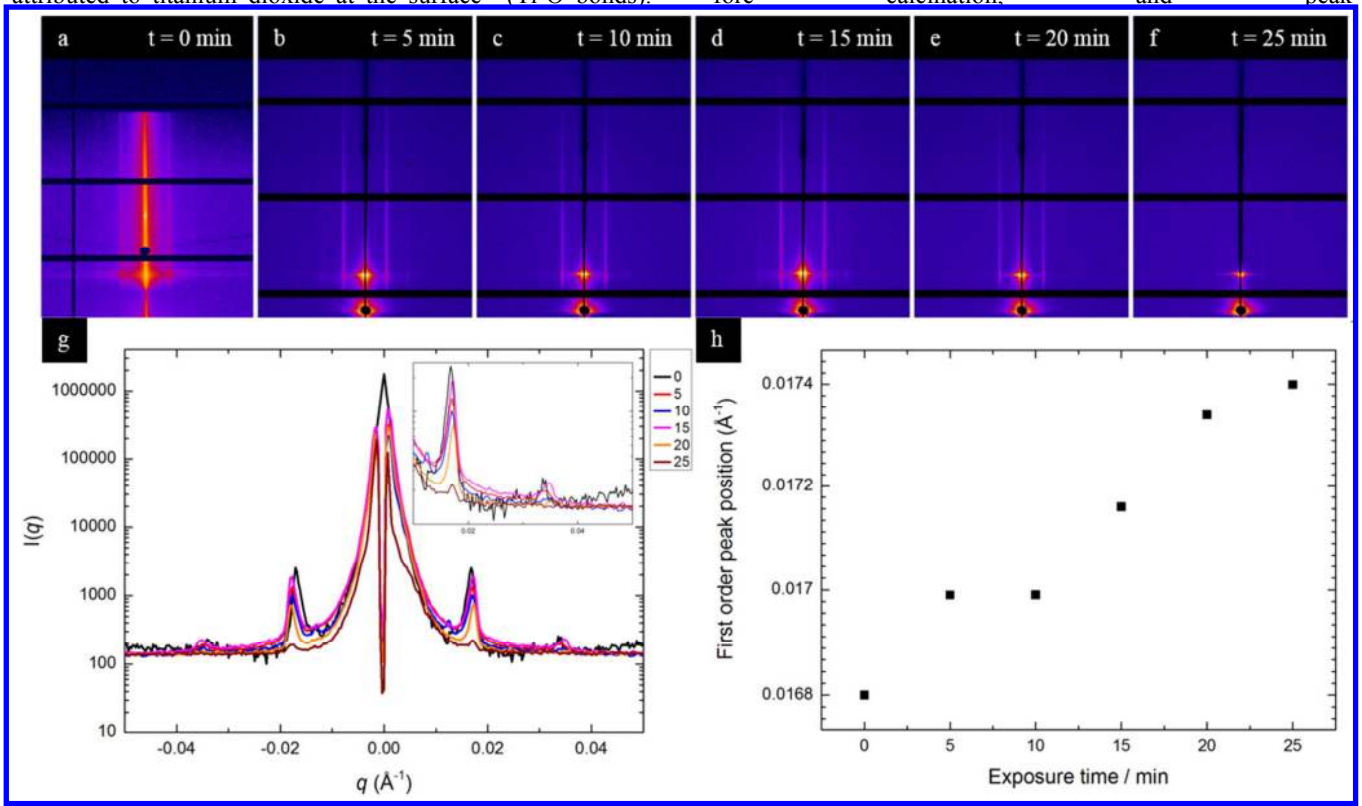

Figure 4. Experiment recorded on titanium dioxide nanowires made at 30 °C, under 60 RH, after UV ozone treatment. 2D-GISAXS patterns of (a) self-assemble BCP thin film, and titanium dioxide nanowires after an exposure time to TTIP of (b) 5 min, (c) 10 min, (d) 15 min, (e) 20 min and (f) 25 minutes respectively. Intensity profile (g) showing peak intensity as a function of q, at various time. Evolution of the first peak order (h) as a function of exposure time.

Influence of the temperature on titanium precursor deposition. Under ambient conditions, well-defined amorphous TiO_2 nanostructures were obtained after 2 hours and up to 4 hours of TTIP exposure (**Figure S3**). Evaporation and incorporation processes can be accelerated and optimized by changing the working temperature. At fixed relative humidity, increasing the temperature from room temperature to 30 °C enhances TTIP evaporation rate due to higher vapor pressure. Also, it decreases effective exposure time needed to form titanium dioxide nanowires dramatically from hours (**Figure S3**) to minutes (e.g. **Figure 3h**). At 40 °C (**Figure S4**), however, the hydrolysis rate of TTIP is too high and it is not possible to generate TiO_2 nanostructures reproducibly. Further, it was not possible to achieve selective incorporation within the PEO domains, leading to overfilling and increased surface roughness. Due to the faster evaporation rate, there is a competition between selective incorporation into the PEO domains and gas-phase reaction between TTIP and water vapors before reaching the substrate[49]. Additional data on the evolution of nanowires fabricated at 40 °C is available in the supplementary information (**Figure S4**).

Influence of relative humidity on titanium precursor deposition. SEM images (**Figure 3**) show the evolution of titanium dioxide formation as a function of relative humidity (y-axis) and exposure time (x-axis) at fixed temperature of 30 °C. Images were taken after exposure to UV ozone for 3 hours. Low relative humidity values (under 40 RH), lowering "air moisture", requires longer exposure time to form well-defined TiO_2 as shown in **Figure 3 (m-p)**: after 5 minutes exposure, no nanostructures are observed at 30 RH. To form nanostructures after a short exposure to TTIP vapors, it is necessary to increase the relative humidity: higher water content favors TTIP hydrolysis and evaporation while enhancing Ti–O bond formation[49]. In **Figure 3 (i-l)** and **(e-h)**, 50 and 60 RH respectively, nanowires formation is observed after 5 min exposure to TTIP. Although, best results are obtained after longer exposure time of 15 - 20 minutes. At high relative humidity values, 70 RH and above, the substrate tends to overfill, and nanowires are not well defined. Sometimes, a titanium dioxide film covering the surface can be observed: chemical reaction between the precursor and water molecules occur in the gas state prior to deposition (**Figure S4**). Such a phenomenon is

beginning to be visible for longer exposure time at 70 RH as shown in **Figure 3 (d).**

These observations give information about the existence of an optimized processing window for the formation of titanium dioxide nanowires. **Figure 3 (l)**, surrounded by an orange border, shows well-defined nanowires obtained after 20 minutes of exposure to TTIP at 30 °C and 50 RH.

For more quantitative information regarding TiO_2 nanowires incorporation, Grazing Incidence Small Angle X-Ray Scattering (GISAXS) was performed. **Figure 4 (a-e)** shows the GISAXS data for samples exposed to TTIP vapors at 30 °C, 60 RH for 5 - 25 minutes. The corresponding SEM images are available in **Figure 3 (e)-(h)**, excluding 25 minutes of exposure. Note that **Figure 4 (a)** is the starting reference for the experiment showing a native self-assembled PS-*b*-PEO thin film, prior to TTIP exposure. The two-dimensional GISAXS patterns presented in

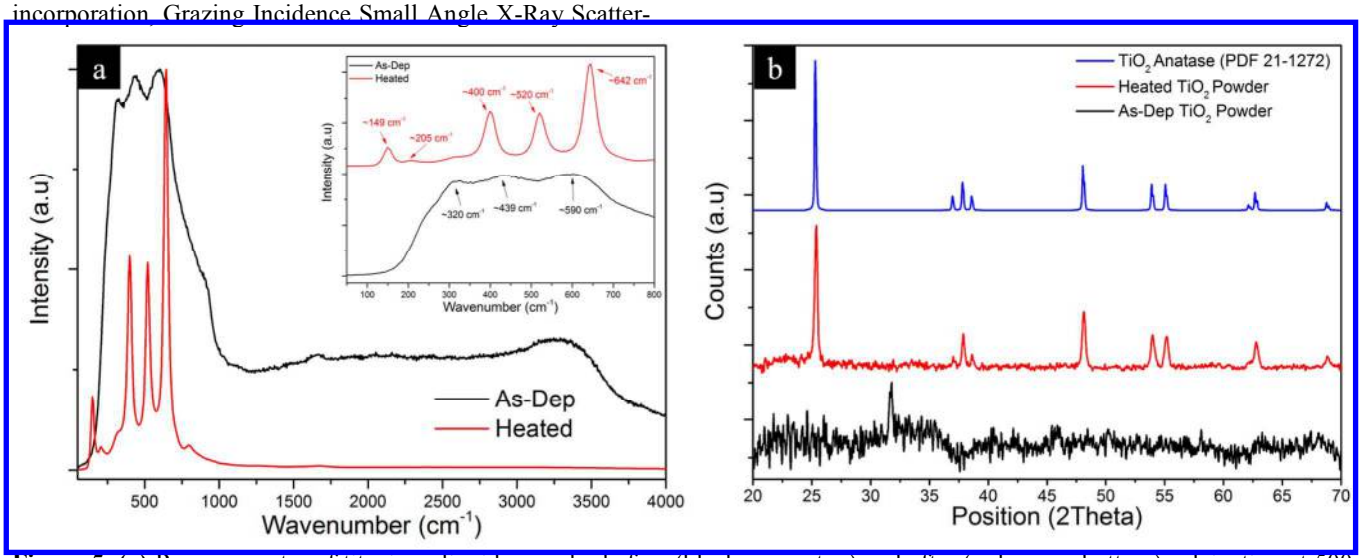

Figure 5. **(a)** Raman spectra of titanium dioxide powder before (black curve, top) and after (red curve, bottom) calcination at 500 °C, showing the intensity as a function of wavenumber. **(b)** XRD spectra of titanium dioxide powder before (black curve, bottom), after (red curve, middle) calcination, and according to PDF 21-1271 anatase (blue curve, top)

Figure 4 (a-h) exhibit strong scattering features perpendicularly orientated to the substrate surface, corresponding to cylinder domains aligned parallel to the substrate. By increasing the TTIP exposure time, initially the intensity of the first order peak increases (**Figure 4 b-d**) and reaches a maximum after 15 minutes (**Figure 4d**). However, when increasing the exposure time further and beyond 20-25 minutes, the intensity of the first order peak becomes significantly weaker, **Figure 4 (e-f)**. We believe this reflects that in the initial part of the process, the reaction of TTIP forms a significant amount of titanium on the PEO domains (before being oxidized to TiO_2 after UV/O_3 treatment). After 15 minutes a saturation point is reached, and the intensity of the first order peak scattering diminishes as titanium hydroxides covers both PEO and PS domains. Meanwhile, a second order peak is observed, in **Figure 4 (b-d)**, for exposure times of 5, 10 and 15 minutes. This peak disappears after 15 minutes exposure to TTIP. Hence, the order of the titanium dioxide nanowires remains improved until 15 minutes of exposure. **Figure 4 (g)** presents the horizontal integrated scattering with the corresponding first and second order position. The position of the first order scattering peak shifts from ~0.0168 to ~0.0174 $Å^{-1}$, as shown in **Figure 4 (h)**, corresponding to 37.3 and 36.1 nm respectively. This domain spacing correlates well with the AFM data of the PS-*b*-PEO template shown in **Figure 1**, where the repeat distance of the PEO domains was ~38 nm.

The SEM data provided in **Figure 3 (e-h, l)** together with the corresponding GISAXS data in **Figure (a-g)** reinforce the effectiveness of this simple CVD-based evaporation method to pattern TiO_2 features. A green border on **Figure (g, h)** highlights the optimum process window to form TiO_2 nanowires: 30 °C, 60 RH and 15 – 20 minutes exposure to TTIP.

Calcination and recrystallization of amorphous titanium dioxide nanostructures. The last stage of this CVD-based method involves calcination of the sample at 500 °C to (a) remove any remaining organic component and (b) convert the titanium dioxide phase from amorphous to anatase. Due to the processing conditions to obtain titanium dioxide nanostructures (low temperature, ambient relative humidity), the TiO_2 nanowires fabricated here are most likely to be amorphous in nature[50]. Following calcination at 500 °C for two hours, titanium dioxide nanowire phases were analyzed *via* Raman spectroscopy and XRD. However, because of their small size, analysis was inconclusive. To address the issue, TTIP was drop-cast onto a glass substrate, left to dry and calcined under the same conditions to mimic the ambient processing conditions of this CVD-based approach. **Figure 5 (a)** and **(b)** represent the phase change from amorphous to crystalline in drop-cast samples as observed with **(a)** Raman spectroscopy and **(b)** XRD analysis.

A 514 nm 30 mW Argon Ion laser selected as the excitation source of the UV Raman spectra, **Figure 5 (a)**. As expected, before calcination, a broad shoulder at 225 cm^{-1} is observed with broad bands at 320, 439 and 590 cm^{-1} indicating the amorphous nature of the sample (TiO_2). After calcination, the Raman spectra shows major bands at 149, 205, 400, 520 and 642 cm^{-1} can be attributed to the Raman-active modes of anatase phase[51,52]. The change from amorphous to anatase is also confirmed *via* XRD analysis, **Figure 5 (b)**. No peaks are observed before calcination (amorphous phase, black curve in **Figure 5b**). When calcined at 500 °C, narrow anatase diffraction peaks at 2θ = 25.3°, 37.0°, 37.8°, 38.6°, 48.1°, 53.9°, 55.1° and 62.87° were observed (red line in Figure **5b**). The-

ses peaks represent the (101), (103), (004), (112), (200), (105), (211), and (213) planes of the anatase phase respectively and match the anatase standard values of the XRD pattern JCPDS no. 21-1272 (shown in blue in Figure **5b**). Although Raman and XRD spectra were recorded on titanium dioxide power, we cautiously believe that our titanium dioxide nanowires will have the same crystalline phase i.e. anatase.

Alongside the phase change from amorphous to crystalline, the calcination process was also used to test the thermal stability of the titanium dioxide nanowires formed. GISAXS was performed on titanium dioxide nanowires before and after the calcination process (**Figure S5**). Data show that the overall order of the system increases after calcination, with an increase in the intensity of the first order scattering peak and a second order scattering peak becoming visible. Additionally, there is a small shift in the position of the first order peak (0.01724 to 0.01709 $Å^{-1}$), which is ascribed to a small increase in the domain spacing and a reduction in nanowire width, consistent with high temperature densification.

CONCLUSIONS

In summary, this work demonstrates how block copolymer thin films may be used to template the formation of titanium dioxide nanostructure *via* exposure to alkoxide precursor vapors followed by subsequent oxidization. This CVD-based approach decouples thin film ordering from titanium dioxide deposition to design the geometry of the initial PS-*b*-PEO pattern and, hence, the resulting titanium dioxide structure. Pattern arrangement and size is intrinsically dependent on the molecular weight and the relative volume fraction of the block copolymer used.

Titanium dioxide was selectively deposited into the hydrophilic block, PEO, utilizing low temperature (from ambient temperature to 40 °C) and a well-known CVD-inspired chemistry: titanium tetraisopropoxide (TTIP) and water as precursors. The quantity of water introduced in the system was controlled by the relative humidity present in the chamber, which was modified from 20 to 70 RH. Alongside the relative humidity, the quality of the titanium dioxide nanostructures was tunable as a function of exposure time to TTIP and temperature. SEM images and GISAXS data suggest the existence of an optimal process window that provides the best ordered pattern: 30 °C, 60 RH, and 15 minutes exposure to TTIP. XPS data taken after UV/ozone treatment confirm the presence of titanium dioxide. Further XPS data, taken after calcination at 500 °C for 2 hours, show that all PEO and polymer matrix are removed. Because titanium dioxide nanowires obtained were small (~24 nm in diameter), Raman and XRD analysis were carried out on pure calcined drop-casted TTIP exposed using the same processing conditions. Both Raman and XRD data confirmed the phase transformation of TiO_2 nanowires from amorphous to anatase after calcination.

Compared to ALD and CVD approaches, this evaporation-based process operates at a much lower temperature and is free from costly equipment and complex processing. Compared to sol-gel techniques used to form titanium dioxide, this approach is more user and environmentally-friendly as there is no need to prepare a metal precursor solution *i.e.* TTIP is used pure and no solvent (ethanol, methanol, etc.) is utilized. Furthermore, additional calcination fully removes the remaining organic mask, and most likely crystallizes amorphous titanium dioxide to anatase without any loss of order. We believe that the evaporation-based approach demonstrated here is a suitable technique for selective deposition at low temperature and a safe environment to produce a large variety of oxides. With the titanium dioxide nanostructures being a few nanometers high after pattern transfer, those nanostructures are fit for industrial purposes, notably in the solar cell industry and gas sensor. A further advantage of our process is the short process time (less than two hours) for microphase separation of the block copolymer thin film ~~to~~ followed by the calcination of the titanium dioxide nanostructures.

EXPERIMENTAL

Materials. Highly polished single-crystal silicon <100> wafers (p-type) with a native oxide layer (~2-5 nm) were used as a substrate. No attempt was taken to remove the native oxide. Wafers were cleaned by ultrasonication in acetone and toluene respectively for 20 min and dried with a nitrogen stream prior to deposition of the BCP *via* spincoating. PS-*b*-PEO was purchased from Polymer Source Inc. (Dorval, Canada) and used without any further purification. (Mn_{PS} = 42 kg mol^{-1}, Mn_{PEO} = 11.5 kg mol^{-1} where Mn is the number average molecular weight, PDI = 1.07 where PDI is the polydispersity index). Titanium tetraisopropoxide (TTIP, 97%), titanium butoxide (TB), toluene (HPLC grade, 99.9%), acetone (HPLC grade, ≥ 99.8%) were purchased from Sigma-Aldrich and used as received.

Template and titanium dioxide formation. *Block-copolymer solution preparation, deposition and pattern formation:* Solutions of PS-*b*-PEO were made in toluene (1 wt%) and stirred for at least 1 hour prior to use. Following dissolution, PS-*b*-PEO thin films were formed by spincoating the 1 wt% BCP solution at 3000 rpm for 30 s onto Si wafer, using a SCS G3P-8 spincoater. Post deposition, the as-cast films were solvent annealed. Films were placed in a 150 mL closed glass jar with a small vial containing 3 mL of toluene and annealed at 60 °C. Line formation (a single row of parallel hexagonally arranged PEO cylinders in a PS matrix) was induced with a 2-hour annealing time.

Titanium dioxide nanostructure formation: Samples were attached upside-down at the top of a 15 mL-closed glass vial (height = 50 mm, diameter = 24 mm) containing 1 mL of titanium tetraisopropoxide. Exposure to TTIP vapors results in the formation of titanium hydroxides and was conducted under ambient temperature (~ 18 °C), 30 °C and 40 °C for time intervals ranging from 5 minutes to 4 hours. In addition, to study the influence of humidity on the evaporation rate of TTIP and subsequent nanostructures formation, the vials were placed in a relative humidity-controlled chamber where relative humidity varied between 20 and 70 RH. The deposited titanium hydroxide nanostructures were oxidized to form titanium dioxide *via* UV/ozone treatment for 3 hours (PSD Pro Series Digital UV/Ozone System; Novascan Technologies, Inc., USA). UV/ozone treatment was also used to ensure the stability of the nanostructures. Samples were then subjected to high temperature (400 to 800 °C) for 2 to 4 hours with 1 and 5 °C /min ramp, resulting in calcination and altering to promote the formation of the anatase phase of titanium dioxide. Shown results are obtained after calcination at 500 °C.

Characterization. BCP film thicknesses were measured using a spectroscopic ellipsometer "Plasmos SD2000 Ellipsometer" at a fixed angle of 70 °C on at least five different places on the sample and was reported as the film thickness result. A two-layer model (SiO_2 + BCP) was used to simulate experimental data. Surface morphologies of the nanostructured thin films

were analyzed with an AFM (Park systems, XE-100) in tapping mode under ambient conditions using silicon microcantilever probes tips with a force constant of 42 N.m-1. Topographic, phase and amplitude images were recorded simultaneously. AFM was used to ensure the quality of the film before titanium dioxide nanostructure formation. SEM measurements were carried out on a JEOL model FEI FP 2031/11 Inspect F field emission at an accelerating voltage of 10 or 20 kV. X-Ray Photoelectron Spectroscopy (XPS) was performed on VG Scientific ECSAlab Mk II system using Al Kα mono X-ray source (1486.6 eV). XPS analysis was used to inform about the chemical state of the titanium. Raman scattering spectroscopy was collected with a Renishaw InVia Raman spectrometer equipped with a 2400 lines/mm grating using a 514 nm 30 mW Argon Ion laser, spectra were collected using a RenCam CCD camera. The beam was focused onto the samples using either a 20x/50x objective lens. The laser power density was adjusted to ensure that the thin film surfaces did not undergo sample heating during the full spectral acquisition time. X-Ray Diffraction (XRD) analysis was performed using a Phillips Xpert PW3719 diffractometer using Cu Kα radiation. (Cu Kα, λ = 0.15418 nm, operation voltage 40 kV, current 40 mA). Grazing-Incidence Small-Angle X-ray Scattering (GISAXS) was performed at beamline I07 and I22, Diamond Light Source Ltd (Didcot, Oxfordshire, UK).

ASSOCIATED CONTENT

Supporting information accompanies this paper to show the application of the process to the formation of TiO_2 nanodots, the evolution of TiO_2 nanowires at various TTIP exposure time at room temperature and 40 °C, and the intensity profile of TiO_2 (GISAXS) after calcination.

AUTHOR INFORMATION

Corresponding Author

* E-mail: mokariap@tcd.ie

Author Contributions

The manuscript was written through contributions of all authors. All authors have given approval to the final version of the manuscript.

Funding Sources

We acknowledge financial support from the Science Foundation Ireland AMBER grant 12/RC/2278 and Semiconductor Research Corporation (SRC) grant 2013-OJ-2444.

ACKNOWLEDGMENT

We would like to thank Diamond Light Source for providing beam time under Allocations SI10439 and SI9328 at lines I07 & I22. We gratefully acknowledge the staff of the Advanced Microscopy Laboratory (AML), Trinity College Dublin, for their assistance for characterization. The authors thanks Dr Colm Glynn and Elaine Carroll for assistance with Raman data.

ABBREVIATIONS

BCP, block copolymer; PS-*b*-PMMA, polystyrene-b-poly(methyl methacrylate); PS-*b*-PEO, polystyrene-b-poly(ethylene oxide); TTIP, titanium tetraisopropoxide; RH, relative humidity

REFERENCES

(1) Varghese, O. K.; Gong, D.; Paulose, M.; Ong, K. G.; Grimes, C. A. Hydrogen Sensing Using Titania Nanotubes. *Sens. Actuators B Chem.* **2003**, *93* (1–3), 338–344.

(2) Zhu, Y.; Shi, J.; Zhang, Z.; Zhang, C.; Zhang, X. Development of a Gas Sensor Utilizing Chemiluminescence on Nanosized Titanium Dioxide. *Anal. Chem.* **2002**, *74* (1), 120–124.

(3) Adachi, M.; Murata, Y.; Okada, I.; Yoshikawa, S. Formation of Titania Nanotubes and Applications for Dye-Sensitized Solar Cells. *J. Electrochem. Soc.* **2003**, *150* (8), G488–G493.

(4) Nedelcu, M.; Lee, J.; Crossland, E. J. W.; Warren, S. C.; Orilall, M. C.; Guldin, S.; Hüttner, S.; Ducati, C.; Eder, D.; Wiesner, U. Block Copolymer Directed Synthesis of Mesoporous TiO2 for Dye-Sensitized Solar Cells. *Soft Matter* **2008**, *5* (1), 134–139.

(5) Langlet, M.; Kim, A.; Audier, M.; Guillard, C.; Herrmann, J. M. Transparent Photocatalytic Films Deposited on Polymer Substrates from Sol–gel Processed Titania Sols. *Thin Solid Films* **2003**, *429* (1–2), 13–21.

(6) Guan, Z.-S.; Zhang, X.-T.; Ma, Y.; Cao, Y.-A.; Yao, J.-N. Photocatalytic Activity of TiO2 Prepared at Low Temperature by a Photo-Assisted Sol-Gel Method. *J. Mater. Res.* **2001**, *16* (04), 907–909.

(7) He, J.; Zhou, W.; Zhou, X.; Zhong, X.; Zhang, X.; Wan, P.; Zhu, B.; Chen, W. The Anatase Phase of Nanotopography Titania Plays an Important Role on Osteoblast Cell Morphology and Proliferation. *J. Mater. Sci. Mater. Med.* **2008**, *19* (11), 3465–3472.

(8) Ahmad, M. I.; Fasel, C.; Mayer, T.; Bhattacharya, S. S.; Hahn, H. High Temperature Stability of Nanocrystalline Anatase Powders Prepared by Chemical Vapour Synthesis under Varying Process Parameters. *Appl. Surf. Sci.* **2011**, *257* (15), 6761–6767.

(9) Shi, J.; Wang, X. Growth of Rutile Titanium Dioxide Nanowires by Pulsed Chemical Vapor Deposition. *Cryst. Growth Des.* **2011**, *11* (4), 949–954.

(10) Halary, E.; Benvenuti, G.; Wagner, F.; Hoffmann, P. Light Induced Chemical Vapour Deposition of Titanium Oxide Thin Films at Room Temperature. *Appl. Surf. Sci.* **2000**, *154–155*, 146–151.

(11) Agafonov, A. V.; Vinogradov, A. V. Sol–gel Synthesis, Preparation and Characterization of Photoactive TIO2 with Ultrasound Treatment. *J. Sol-Gel Sci. Technol.* **2009**, *49* (2), 180–185.

(12) Wang, C.-C.; Ying, J. Y. Sol−Gel Synthesis and Hydrothermal Processing of Anatase and Rutile Titania Nanocrystals. *Chem. Mater.* **1999**, *11* (11), 3113–3120.

(13) Major, B.; Ebner, R.; Zieba, P.; Wolczynski, W. Titanium-Based Films Deposited Using a Nd:YAG Pulsed Laser. *Appl. Phys. A* **1999**, *69* (1), S921–S923.

(14) Potts, S. E.; Profijt, H. B.; Roelofs, R.; Kessels, W. M. M. Room-Temperature ALD of Metal Oxide Thin Films by Energy-Enhanced ALD. *Chem. Vap. Depos.* **2013**, *19* (4–6), 125–133.

(15) Ratzsch, S.; Kley, E.-B.; Tünnermann, A.; Szeghalmi, A. Influence of the Oxygen Plasma Parameters on the Atomic Layer Deposition of Titanium Dioxide. *Nanotechnology* **2015**, *26* (2), 024003.

(16) Ritala, M.; Leskela, M.; Niinisto, L.; Haussalo, P. Titanium Isopropoxide as a Precursor in Atomic Layer Epitaxy of Titanium Dioxide Thin Films. *Chem. Mater.* **1993**, *5* (8), 1174–1181.

(17) Sinha, A.; Hess, D. W.; Henderson, C. L. Area Selective Atomic Layer Deposition of Titanium Dioxide: Effect of Precursor Chemistry. *J. Vac. Sci. Technol. B* **2006**, *24* (6), 2523–2532.

(18) van de Krol, R.; Goossens, A. Structure and Properties of Anatase TiO2 Thin Films Made by Reactive Electron Beam Evaporation. *J. Vac. Sci. Technol. Vac. Surf. Films* **2003**, *21* (1), 76.

(19) Matsen, M. W.; Bates, F. S. Unifying Weak- and Strong-Segregation Block Copolymer Theories. *Macromolecules* **1996**, *29* (4), 1091–1098.

(20) Erothu, H.; Kolomanska, J.; Johnston, P.; Schumann, S.; Deribew, D.; Toolan, D. T. W.; Gregori, A.; Dagron-Lartigau, C.; Portale, G.; Bras, W. Synthesis, Thermal Processing, and Thin Film Morphology of Poly(3-hexylthiophene)–Poly(styrenesulfonate) Block Copolymers. *Macromolecules* **2015**, *48* (7), 2107–2117.

(21) Borah, D.; Rasappa, S.; Senthamaraikannan, R.; Kosmala, B.; Shaw, M. T.; Holmes, J. D.; Morris, M. A. Orientation and Alignment Control of Microphase-Separated PS- *B* -PDMS Substrate Patterns via Polymer Brush Chemistry. *ACS Appl. Mater. Interfaces* **2013**, *5* (1), 88–97.

(22) Cummins, C.; Ghoshal, T.; Holmes, J. D.; Morris, M. A. Strategies for Inorganic Incorporation Using Neat Block Copolymer

Thin Films for Etch Mask Function and Nanotechnological Application. *Adv. Mater.* **2016**, *28* (27), 5586–5618.

(23) Gutierrez, J.; Tercjak, A.; Garcia, I.; Peponi, L.; Mondragon, I. Hybrid Titanium Dioxide/PS-B-PEO Block Copolymer Nanocomposites Based on Sol–gel Synthesis. *Nanotechnology* **2008**, *19* (15), 155607.

(24) Cha, M.-A.; Shin, C.; Kannaiyan, D.; Jang, Y. H.; Kochuveedu, S. T.; Ryu, D. Y.; Kim, D. H. A Versatile Approach to the Fabrication of TiO2nanostructures with Reverse Morphology and Mesoporous Ag/TiO2 Thin Films via Cooperative PS-B-PEO Self-Assembly and a Sol-Gel Process. *J. Mater. Chem.* **2009**, *19* (39), 7245–7250.

(25) Gutierrez, J.; Tercjak, A.; Mondragon, I. Conductive Behavior of High TiO2 Nanoparticle Content of Inorganic/Organic Nanostructured Composites. *J. Am. Chem. Soc.* **2010**, *132* (2), 873–878.

(26) Agarwala, S.; Ho, G. W. Synthesis and Tuning of Ordering and Crystallinity of Mesoporous Titanium Dioxide Film. *Mater. Lett.* **2009**, *63* (18–19), 1624–1627.

(27) Yoshida, M.; Prasad, P. N. Sol−Gel-Processed SiO2/TiO2/Poly(vinylpyrrolidone) Composite Materials for Optical Waveguides. *Chem. Mater.* **1996**, *8* (1), 235–241.

(28) Boettcher, S. W.; Fan, J.; Tsung, C.-K.; Shi, Q.; Stucky, G. D. Harnessing the Sol–Gel Process for the Assembly of Non-Silicate Mesostructured Oxide Materials. *Acc. Chem. Res.* **2007**, *40* (9), 784–792.

(29) Brezesinski, T.; Groenewolt, M.; Gibaud, A.; Pinna, N.; Antonietti, M.; Smarsly, B. Evaporation-Induced Self-Assembly (EISA) at Its Limit: Ultrathin, Crystalline Patterns by Templating of Micellar Monolayers. *Adv. Mater.* **2006**, *18* (17), 2260–2263.

(30) Ghoshal, T.; Maity, T.; Godsell, J. F.; Roy, S.; Morris, M. A. Large Scale Monodisperse Hexagonal Arrays of Superparamagnetic Iron Oxides Nanodots: A Facile Block Copolymer Inclusion Method. *Adv. Mater.* **2012**, *24* (18), 2390–2397.

(31) Ghoshal, T.; Shaw, M. T.; Bolger, C. T.; Holmes, J. D.; Morris, M. A. A General Method for Controlled Nanopatterning of Oxide Dots: A Microphase Separated Block Copolymer Platform. *J. Mater. Chem.* **2012**, *22* (24), 12083–12089.

(32) Mayeda, M. K.; Hayat, J.; Thomas H Epps, I. I. I.; Lauterbach, J. Metal Oxide Arrays from Block Copolymer Thin Film Templates. *J. Mater. Chem. A* **2015**, *3* (15), 7822–7829.

(33) Lee, D. H.; Shin, D. O.; Lee, W. J.; Kim, S. O. Hierarchically Organized Carbon Nanotube Arrays from Self-Assembled Block Copolymer Nanotemplates. *Adv. Mater.* **2008**, *20* (13), 2480–2485.

(34) Peng, Q.; Tseng, Y.-C.; Darling, S. B.; Elam, J. W. A Route to Nanoscopic Materials via Sequential Infiltration Synthesis on Block Copolymer Templates. *ACS Nano* **2011**, *5* (6), 4600–4606.

(35) Peng, Q.; Tseng, Y.-C.; Darling, S. B.; Elam, J. W. Nanoscopic Patterned Materials with Tunable Dimensions via Atomic Layer Deposition on Block Copolymers. *Adv. Mater.* **2010**, *22* (45), 5129–5133.

(36) Peng, Q.; Tseng, Y.-C.; Long, Y.; Mane, A. U.; DiDona, S.; Darling, S. B.; Elam, J. W. Effect of Nanostructured Domains in Self-Assembled Block Copolymer Films on Sequential Infiltration Synthesis. *Langmuir* **2017**, *33* (46), 13214–13223.

(37) Thomas, S.; Grohens, Y.; Jyotishkumar, P. *Characterization of Polymer Blends: Miscibility, Morphology and Interfaces*; John Wiley & Sons, 2014.

(38) Hansen, C. M. *Hansen Solubility Parameters: A User's Handbook, Second Edition*; CRC Press, 2007.

(39) Auras, R. A.; Lim, L.-T.; Selke, S. E. M.; Tsuji, H. *Poly(lactic Acid): Synthesis, Structures, Properties, Processing, and Applications*; John Wiley & Sons, 2011.

(40) Besley, L. M.; Bottomley, G. A. Vapour Pressure of Toluence from 273.15 to 298.15 K. *J. Chem. Thermodyn.* **1974**, *6* (6), 577–580.

(41) Mokarian-Tabari, P.; Collins, T. W.; Holmes, J. D.; Morris, M. A. Cyclical "Flipping" of Morphology in Block Copolymer Thin Films. *ACS Nano* **2011**, *5* (6), 4617–4623.

(42) Woodley, D. M.; Dam, C.; Lam, H.; LeCave, M.; Devanand, K.; Selser, J. C. Draining and Long-Ranged Interactions in the Poly(ethylene Oxide)/Water Good Solvent System. *Macromolecules* **1992**, *25* (20), 5283–5286.

(43) Rawolle, M.; Ruderer, M. A.; Prams, S. M.; Zhong, Q.; Magerl, D.; Perlich, J.; Roth, S. V.; Lellig, P.; Gutmann, J. S.; Müller-Buschbaum, P. Nanostructuring of Titania Thin Films by a Combination of Microfluidics and Block-Copolymer-Based Sol–Gel Templating. *Small* **2011**, *7* (7), 884–891.

(44) Mahshid, S.; Askari, M.; Ghamsari, M. S. Synthesis of TiO2 Nanoparticles by Hydrolysis and Peptization of Titanium Isopropoxide Solution. *J. Mater. Process. Technol.* **2007**, *189* (1–3), 296–300.

(45) Tsvetanov, C. B.; Stamenova, R.; Dotcheva, D.; Doytcheva, M.; Belcheva, N.; Smid, J. Intelligent Networks Based on Poly(oxyethylene). *Macromol. Symp.* **1998**, *128* (1), 165–182.

(46) Bullock, E. L.; Patthey, L.; Steinemann, S. G. Clean and Hydroxylated Rutile TiO2(110) Surfaces Studied by X-Ray Photoelectron Spectroscopy. *Surf. Sci.* **1996**, *352–354*, 504–510.

(47) Briggs, D. Handbook of X-Ray Photoelectron Spectroscopy C. D. Wanger, W. M. Riggs, L. E. Davis, J. F. Moulder and G. E.Muilenberg Perkin-Elmer Corp., Physical Electronics Division, Eden Prairie, Minnesota, USA, 1979. 190 Pp. $195. *Surf. Interface Anal.* **1981**, *3* (4), v–v.

(48) Liu, F.-M.; Wang, T.-M. Surface and Optical Properties of Nanocrystalline Anatase Titania Films Grown by Radio Frequency Reactive Magnetron Sputtering. *Appl. Surf. Sci.* **2002**, *195* (1–4), 284–290.

(49) Fuyuki, T.; Kobayashi, T.; Matsunami, H. Effects of Small Amount of Water on Physical and Electrical Properties of TiO2 Films Deposited by CVD Method. *J. Electrochem. Soc.* **1988**, *135* (1), 248–250.

(50) Mathews, N. R.; Morales, E. R.; Cortés-Jacome, M. A.; Toledo Antonio, J. A. TiO2 Thin Films - Influence of Annealing Temperature on Structural, Optical and Photocatalytic Properties. *Sol. Energy* **2009**, *83* (9), 1499–1508.

(51) Ohsaka, T.; Izumi, F.; Fujiki, Y. Raman Spectrum of Anatase, TiO2. *J. Raman Spectrosc.* **1978**, *7* (6), 321–324.

(52) Zhang, J.; Li, M.; Feng, Z.; Chen, J.; Li, C. UV Raman Spectroscopic Study on TiO2. I. Phase Transformation at the Surface and in the Bulk. *J. Phys. Chem. B* **2006**, *110* (2), 927–935.

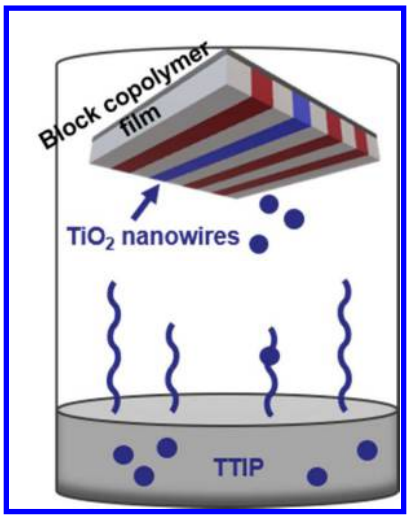

Figure 6. For Table of Content Only